Pergamon

Int. J. Heat Mass Transfer. Vol. 38, No. 5, pp. 887–897, 1995

0017–9310/95 $9.50+0.00

0017–9310(94)00200–2

Heat transfer within a concrete slab with a finite microwave heating source

L. E. LAGOS, W. LI and M. A. EBADIAN†
Department of Mechanical Engineering, Florida International University, Miami, FL 33199, U.S.A.

and

T. L. WHITE,‡ R. G. GRUBB and D. FOSTER§
‡Fusion Energy Division, §Chemical Technology Division, Oak Ridge National Laboratory, Oak Ridge, TN 37831, U.S.A.

(*Received* 28 *October* 1993 *and in final form* 24 *June* 1994)

Abstract—In the present paper, the concrete decontamination and decommissioning process with a finite microwave heating source is investigated theoretically. For the microwave induced heating pattern, a multilayer concrete slab, which includes steel reinforcement mesh, is assumed to be exposed to a finite plane microwave source at normal incidence. Two-dimensional heat transport within the concrete is also considered to evaluate the variations of temperature with heating time at different frequencies with and without the presence of the reinforcement bars. Four commonly used industrial microwave frequencies of 0.896, 2.45, 10.6 and 18.0 GHz have been selected. The results revealed that as the microwave frequency increases to, or higher than 10.6 GHz, the maximum temperature shifts toward the front surface of the concrete. It was found that the presence of a steel reinforcement mesh causes part of the microwave energy to be blocked and reflected. Furthermore, it was observed that the temperature distribution is nearly uniform within the dimensions of the microwave applicator for a high microwave power intensity ($Q_{0,ave} \approx 8.0 \times 10^5$ W m^{-2}) and a short heating time ($t \approx 60$ s).

1. INTRODUCTION

Concrete is a common material used extensively in nuclear engineering for shielding, for nuclear reactor construction, and the buildings around the reactors, for hot cells, waste processing plants, etc. Massive amounts of concrete surfaces and floors in these installations and buildings have been contaminated from nuclear reaction and other related processes. For example, at Oak Ridge National Laboratory (ORNL) alone, there are 50 000 tons of concrete block, and about 2 million m^2 of concrete surface that have been highly contaminated.

In most cases, only the outer surface of the concrete, to a depth of less than a couple of centimeters, is radioactively contaminated. As regulation of nuclear waste management becomes increasingly restrictive, it is expected that only contaminated concrete surfaces or layers will be treated as radioactive waste, while the main bulk of the concrete will be treated as regular waste. In this way, a large number of waste sites could be freed for more waste, thus saving vast sums of money to build more sites. Presently, mechanical techniques are utilized worldwide to separate contaminated concrete surfaces and layers from the bulk concrete. Basically, mechanical techniques have a number of shortcomings. For example, impact breaking machines generate large amounts of dust, and these machines must be operated subject to wet conditions to suppress dust generation, thus, forcing soluble contamination deeper into the concrete. In addition, high-pressure water sprayers produce huge volumes of secondary contaminated water, and some means for recycling the waste water are needed. To a varying extent, all of the mechanical techniques generate dust or waste water, while storage and recycling of these secondary radioactive wastes also engender other problems. Microwave technology has several advantages over conventional mechanical methods, such as minimizing the generation of secondary wastes (water and dust), reducing the cost of system maintenance, and lessening radioactive exposure to the worker during operation.

"Concrete breaking by microwaves" first appeared as the subject of an experimental study in the U.K. by Watson [1]. Great interest was aroused worldwide by this first success, and many applications of this technique have been investigated as an extension of the application of microwave energy for non-communication purposes. Recently, much more emphasis has been placed on the development of techniques for separating radioactively contaminated concrete surfaces from nuclear power plant structures. Several groups [2–7] have begun developing new processes

†Author to whom correspondence should be addressed.

NOMENCLATURE

A	complex constant
B	complex constant
C	complex constant
C_p	specific heat of the concrete [J kg^{-1} K^{-1}]
D	microwave applicator size in the y-direction [m] or complex constant
d	diameter of the steel reinforcement bar [m]
E_0	amplitude of the initial electric field [V m^{-1}]
E_y	electric potential for the plane wave assumption [V m^{-1}]
F	complex constant
f	microwave frequency [Hz]
G	complex constant
H	limitation of the concrete during the calculation [m]
H_z	magnetic potential [A m^{-1}]
j	imaginary number, $\sqrt{-1}$
k_{eff}	effective thermal conductivity [W K^{-1} m^{-1}]
L	thickness of the concrete [m]
L_h	distance between the horizontal steel reinforcement bars [m]
L_s	location of the steel reinforcement mesh [m]
L_v	distance between the vertical steel reinforcement bars [m]
N	total node number
$Q_{d,ave}$	microwave power dissipation [W m^{-3}]
Q_0	time averaged microwave power intensity [W m^{-2}]
q	dimensionless heat generation
Re	real part of the complex value
r	complex constant determined by dielectric properties
T	temperature [°C]
t	time [s]
t_{sm}	fraction of the energy passed through the steel reinforcement, $1-\rho_{sm}$
x, y	coordinates [m]
z	coordinate of the wave propagation direction [m].

Greek symbols

Δ	thickness of the steel reinforcement layer [m]
ε	complex dielectric permittivity, $\varepsilon' - j\varepsilon''_{eff}$ [F m^{-1}]
ε_{air}	dielectric permittivity of air, 8.86×10^{-12} [F m^{-1}]
ε'	real part of the complex dielectric permittivity, or dielectric constant [F m^{-1}]
ε''	imaginary part of the complex dielectric permittivity, or dielectric loss [F m^{-1}]
ε''_{eff}	effective dielectric loss, $\varepsilon'' + \sigma/\omega$ [F m^{-1}]
η	dimensionless coordinate, y/L, or complex constant
θ	dimensionless temperature $(T-T_\infty)/(P_{0,ave}L^2/k)$
λ	wavelength of the microwave [m]
μ	dielectric permeability [H m^{-1}]
μ_{air}	permeability of free-space (air) $4\pi \times 10^{-7}$ [H m^{-1}]
ξ	dimensionless coordinate, x/L
ρ	density [kg m^{-3}]
ρ_{sm}	fraction of the energy reflected from the steel reinforcement, $1-t_{sm}$
σ	dielectric conductivity [Ω^{-1}]
τ	dimensionless time
ω	microwave angle frequency, $2\pi f$ [rad s^{-1}].

Subscript

air	air
max	maximum value
s	steel reinforcement
1	material 1, concrete layer 1 ($0 \leqslant z \leqslant 0.1$ m)
2	material 2, concrete layer 2 (0.1 m $< z \leqslant 0.6$ m).

that use microwave energy for thermally separating contaminated concrete surfaces.

Due to the potential advantages offered by microwave technology, an experimental investigation of concrete decontamination and decommissioning (D&D) was initiated in 1992 [4] at the Oak Ridge National Laboratory (ORNL). The advantages of this new methodology and technology of concrete decontamination using microwave heating have been successfully demonstrated. Experimentally, however, there are too many factors, or parameters, affecting the success of the spalling of the concrete layer and the spalling speed. Therefore, it is almost impossible to consider all of these parameters in an experimental investigation unless there is a willingness to spend a great deal of time and money. As part of the continuing research on the experimental investigation, a group of scientists and engineers from Florida International University and ORNL first initiated a theoretical analysis in 1992 [5–7].

For several decades, scientists and engineers in civil engineering have shown considerable interest in the

problem of heat transfer, fire damage, and related stress analysis in concrete, that affects concrete properties and determines the failure of concrete construction. For example, extensive research on concrete fire damage has been conducted by Harmathy [8], and an excellent review of transient thermal strain is provided in [9]. Recently, Li *et al.* [6] modified their previous conduction model of unsteady heat transfer and thermal stress within the concrete subject to microwave heating [5], and extended their analysis to the unsteady heat and mass transfer of porous concrete with constant dielectric properties for microwave frequencies ranging from 0.896 to 18.0 GHz. As an extension, the effects of the steel reinforcement mesh on temperature and steam pressure within porous concrete have been further analyzed. However, in these previous studies, only one-dimensional heat transfer was considered. During the concrete decontamination and decommissioning (D&D) process, the shape of the microwave applicator is rectangular (109 mm by 54.6 mm). Obviously, a one-dimensional analysis will limit the results and discussion.

For the second phase of this theoretical investigation, a two-dimensional heat transfer model was employed to more closely simulate the concrete D&D process. In the present paper, only heat conduction is considered in the heat transfer analysis. Theoretically, both the dielectric and thermal properties of concrete are functions of the unknown temperature distributions. Thus, the effects of the steel reinforcement mesh on the temperature are also analyzed in the present study. A uniform plane microwave at normal incidence is considered, while the steel reinforcement within the concrete is treated as a thin layer having uniform reflection and transmission.

2. PROBLEM FORMULATION

A full model of concrete decontamination using microwave technology would require a vast number of parameters to be taken into consideration. Principally, an accurate evaluation of the microwave field, which determines heat dissipation within the concrete, is very important.

2.1. *Governing equation of the electromagnetic field*

Generally, microwaves are electromagnetic waves having frequencies ranging from 300 MHz to 300 GHz. Therefore, microwaves satisfy Maxwell's equation, which describes electromagnetic fields. During the decontamination process, the front surface of a concrete slab ($x = 0$) is directly exposed to the microwave source. The steel reinforcement mesh is located at a distance (L_s) from the front surface of the concrete slab with a total thickness (L), as shown in Fig. 1(a). The steel reinforcement within the concrete is treated as an infinite thin layer, and has no dielectric loss ($\varepsilon''_{\text{eff}}{}_s = 0$), and $\mu_s = \mu_{\text{air}}$. The steel layer has a certain dielectric constant, ε'_s, which has a uniform reflection and transmission. The layer thickness (Δ) is very small and might be totally neglected in the heat transfer, except that its certain dielectric properties cause an additional part of the microwave energy to be reflected. The fraction of reflection caused by the steel reinforcement (ρ_{sm}) is assumed to be equal to a fraction of the cross-sectional area of the concrete taken up by the steel mesh. For example, the steel reinforcement mesh consists of steel bars or wire having a diameter (d) with horizontal and vertical spaces (L_h and L_v), as shown in Fig. 1(b). The steel reinforcement reflection (ρ_{am}) equals $[(L_h + L_v)\,d - d^2]/(L_h L_v)$. When $d = 2.5$ cm and $L_h = L_v = 25$ cm, $\rho_{\text{sm}} = 0.19$.

For the constant dielectric properties and the plane wave and propagation in the x-direction, Maxwell's equation can be simplified as

$$\frac{dE_y}{dx} = j\mu\omega H_z, \quad \frac{dH_z}{dx} = -j\omega\varepsilon E_y \tag{1}$$

with boundary conditions of

$$E_{y2} = E_{y1} \quad H_{z2} = H_{z1}. \tag{2}$$

The general solution of these plane wave equations can be obtained as

$$E_y = Ae^{-rx} + Be^{rx} \quad H_z = \frac{1}{\eta}(Ae^{-rx} - Be^{rx}) \tag{3}$$

in which

$$\varepsilon = \varepsilon' - j\varepsilon''_{\text{eff}} \quad r = \sqrt{(j\omega\varepsilon)} \quad \text{and} \quad \eta = j\mu\omega/r. \tag{4}$$

One can now consider a concrete slab consisting of two concrete layers that sandwich the steel reinforcement mesh at the location of $x = L_s$, as shown in Fig. 1(a). The front surface at $x = 0$ is directly exposed to the microwave source. Two concrete layers could have different dielectric properties (μ_1, ε_1 and μ_2, ε_2), but the variation of these properties with the heating process (temperature) is assumed to be constant. As is generally known, the concentration of ferromagnetic material in concrete is negligible. Therefore, the difference in the permeability of the concrete layers (μ_1 and μ_2) and the free-space (air) can also be neglected.

Based on the above assumptions and boundary conditions, the electric and magnetic fields within the concrete can be solved in the following form:

$$E_y = E_0(Ce^{-r_1 x} + De^{r_1 x}) \quad \text{for} \quad 0 \leqslant x < L_s \tag{5}$$

$$H_z = \eta_1^{-1} E_0(Ce^{-r_1 x} - De^{r_1 x}) \quad \text{for} \quad 0 \leqslant x < L_s \tag{6}$$

and

$$E_y = E_0(Fe^{-r_2 x} + Ge^{r_2 x}) \quad \text{for} \quad L_s < x \leqslant L \tag{7}$$

$$H_z = \eta_2^{-1} E_0(Fe^{-r_2 x} - Ge^{r_2 x}) \quad \text{for} \quad L_s < x \leqslant L \tag{8}$$

with

$$C = \frac{2\eta_1[(\eta_3 + \eta_2) - \rho_{\text{sm}}(\eta_3 - \eta_2)e^{-2r_2 L}]}{(\eta_3 + \eta_2)(\eta_1 + \eta_0) + \rho_{\text{sm}}(\eta_3 + \eta_2)(\eta_1 - \eta_0) + (t_{\text{sm}}^2 - \rho_{\text{sm}}^2)(\eta_3 - \eta_2)(\eta_1 - \eta_0)e^{-2r_2 L}} \tag{9}$$

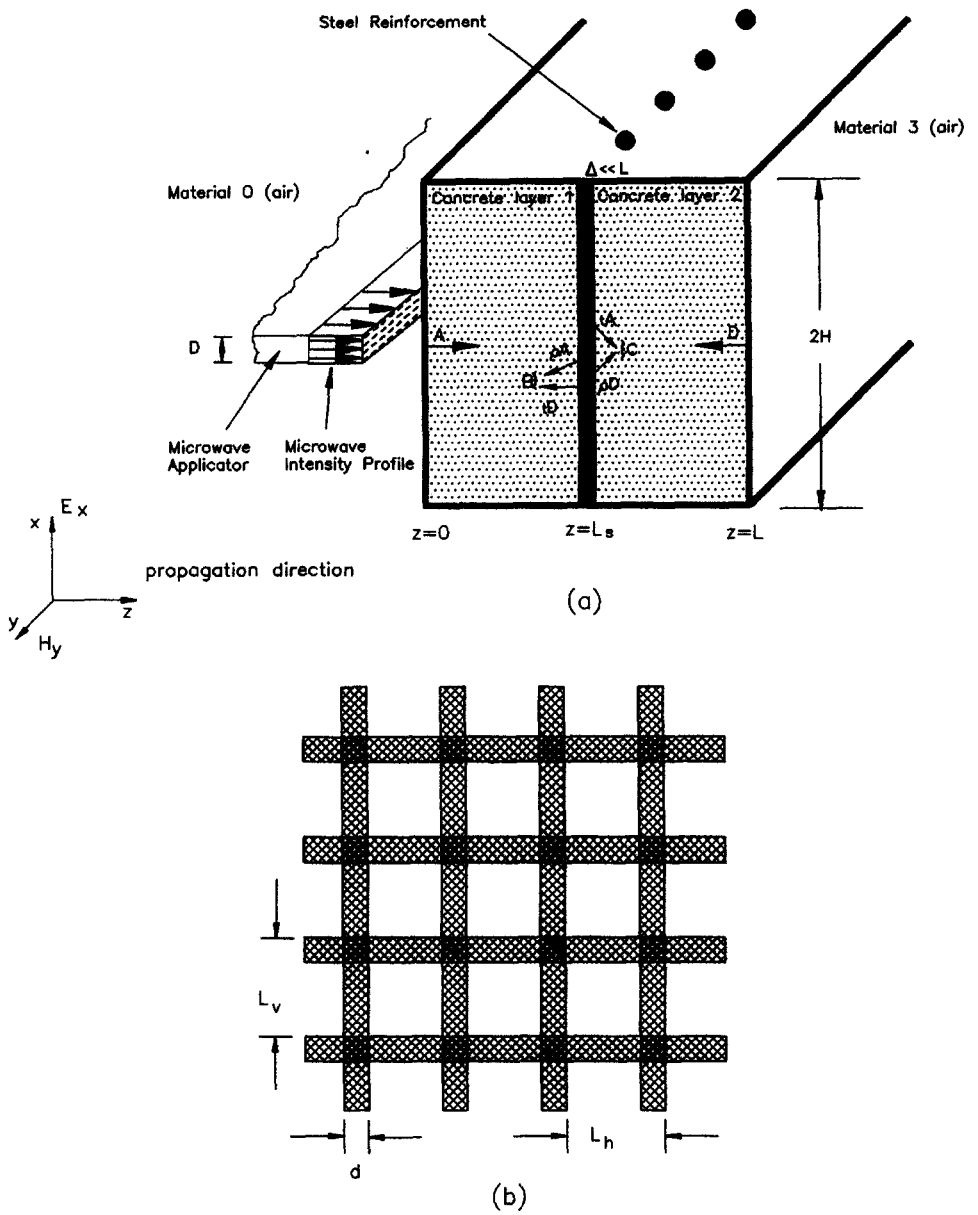

Fig. 1. Geometry of the concrete slab, microwave applicator, and the steel reinforcement mesh. (a) Geometry of the concrete slab and microwave applicator and (b) geometry of the steel reinforcement mesh within the concrete.

$$G = \frac{t_{sm}(\eta_3 - \eta_2)\,e^{-2r_2L}C}{(\eta_3+\eta_2) - \rho_{sm}(\eta_3-\eta_2)e^{-2r_2L}} \tag{10}$$

$$D = \rho_{sm}C + t_{sm}G \tag{11}$$

$$F = t_{sm}C + \rho_{sm}G \tag{12}$$

where E_0 is the wave amplitude determined by the incident power density. Constants r and η, as well as the constants C, D, F and G, are complex values. Thus, the final solution of E_x and H_y is complex.

2.2. *Incident power and power dissipation*

In electric and magnetic fields for the free-space (air) before interfacing with the concrete slab, the time averaged incident power density (Q_0) carried by the microwaves has the following relation with the wave amplitude [10]:

$$Q_0 = [\mathrm{Re}(E_0 e^{i\omega t})]^2/(240\pi). \tag{13}$$

Finally, since the microwave frequencies are very high (from 300 MHz to 300 GHz), the time scale of the sinusoidal variations of the microwave field is much smaller than that of the temperature variations in the concrete. One can then separate the sinusoidal variation of the microwave with the unsteady heat transport phenomena. The time averaged microwave power dissipation ($Q_{d,ave}$) can thus be calculated as

$$Q_{d,ave} = \tfrac{1}{2}(\omega\varepsilon''_{eff})(240\pi Q_0)\|E_y/E_0\|^2 \quad \text{for } |y| < D/2. \tag{14}$$

It should be noted that the time averaged microwave power dissipation ($Q_{d,ave}$) is proportional to the product of the imaginary part of the concrete complex dielectric permittivity (or effective dielectric loss, ε''_{eff}) and the square of the norm of the complex electric field (E_y).

2.3. *Heat transfer within the concrete*

A model for two-dimensional unsteady temperature distribution with constant thermal properties is employed in the current analysis. The energy equation within the concrete slab can be specified as

$$\rho C_p \frac{\partial T(x,y,t)}{\partial t} = k_{eff}\left[\frac{\partial^2 T(x,y,t)}{\partial x^2} + \frac{\partial^2 T(x,y,t)}{\partial y^2}\right] + Q_{d,ave}(x,y) \tag{15}$$

in which T is the temperature within the concrete. $Q_{d,ave}$ is the time averaged microwave power dissipation. ρ, k_{eff} and C_p are the density, effective thermal conductivity, and specific heat of the concrete, respectively, and are assumed to be constants in the current analysis.

2.4. *Boundary and initial conditions for temperature*

The thermal boundary conditions on all concrete walls may be approximately assumed as

$$T = T_\infty \quad \text{at} \quad x = 0 \tag{16}$$

$$T = T_\infty \quad \text{at} \quad x = L \tag{17}$$

$$\frac{\partial T}{\partial y} = 0 \quad \text{at} \quad y = 0 \tag{18}$$

$$T = T_\infty \quad \text{at} \quad y = H. \tag{19}$$

The initial condition of the concrete slab can be specified as

$$T = T_0 \quad \text{at} \quad t = 0 \tag{20}$$

where T_∞ and T_0 are the ambient and initial temperatures, respectively. In the analysis, $T_0 = T_\infty = 20°C$ is used.

3. SOLUTION PROCEDURE

3.1. *Dimensionless parameters*

By introducing the following dimensionless parameters and knowing that $T_\infty = T_0$

$$\theta = \frac{T - T_\infty}{Q_0 T_0} \quad \xi = \frac{x}{L} \quad \eta = \frac{y}{L}$$

$$\tau = \frac{k_{eff} t}{(\rho C_p)_0 L^2} \quad q = \frac{Q_{d,ave} L^2}{Q_0 k_{eff} T_0} \tag{21}$$

the energy equation, and the initial and boundary conditions can be written in the following dimensionless form:

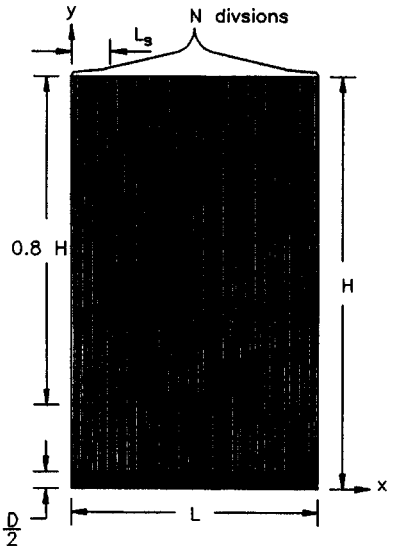

Fig. 2. Mesh generation for two-dimensional finite element calculation.

$$\frac{\partial\theta}{\partial\tau} = \frac{\partial^2\theta}{\partial\xi^2} + \frac{\partial^2\theta}{\partial\eta^2} + q(\xi,\eta) \tag{22}$$

$$\theta = 0 \quad \text{at} \quad \tau = 0 \tag{23}$$

$$\theta = 0 \quad \text{at} \quad \xi = 0 \tag{24}$$

$$\theta = 0 \quad \text{at} \quad \xi = 1 \tag{25}$$

$$\frac{\partial\theta}{\partial\eta} = 0 \quad \text{at} \quad \eta = 0 \tag{26}$$

$$\theta = 0 \quad \text{at} \quad \eta = H/L. \tag{27}$$

As indicated by the dimensionless equations, the dimensionless temperature is directly proportional to the microwave power intensity (Q_0). Therefore, for different values of (Q_0), the dimensionless temperature will have the same temperature distributions. In the analysis, $Q_0 = 8.0 \times 10^5$ W m^{-2} is used as an example to provide a direct sense of the real temperature.

The above governing equation is solved by an implicit finite element method. To ensure that, each wavelength of the microwaves in the concrete, $\lambda \approx 1/[f\sqrt{(\mu_{air}\varepsilon')}] \approx 6.3 \times 10^{-3}$ m for $f = 18.0$ GHz, has more than 10 subdivisions in the numerical calculation. Thus, the total 1500 nodes in the wave propagation direction (x) were used in the analysis.

3.2. *Mesh grid generation*

Generally, two kinds of mesh grids (Type I and Type II) for the finite element method were generated according to the microwave frequencies. In the Type I mesh, 100 nodes in the x-direction were employed for the temperature calculation, see Fig. 2. In the Type II mesh, 150 nodes in the x-direction were utilized for the temperature calculation. In each division for both Type I and Type II meshes, 10 subdivisions were divided for calculating the power dissipation. Therefore, 1000 and 1500 divisions for Type I and Type II, respec-

Table 1. Reference values of the properties of concrete

Properties	Description	Value
Composition	Composition, expressed as ratios to the cement content are:	
	20 mm crushed limestone aggregate	3.19
	sand	2.59
	cement (ordinary Portland)	1.00
	water	0.60
	cement content of concrete	300 kg m^{-3}
	Derivation: ref. [11]	
Density (ρ)	Derivation: ref. [11]	2300 kg m^{-3}
Specific heat (C_p)	Derivation: ref. [12]	650 J kg^{-1} K^{-1}
Thermal conductivity (k)	Derivation: ref. [12]	0.87 W m^{-1} K^{-1}
Relative dielectric permittivity, real part ($\varepsilon'/\varepsilon_0$)	$f = 0.896$ GHz at 25°C	7.94
	$f = 2.45$ GHz at 25°C	6.18
	$f = 10.6$ GHz at 25°C	8.43
	$f = 18.0$ GHz at 25°C	7.46
	Derivation: ref. [13]	
Relative dielectric permittivity, imaginary part ($\varepsilon''_{eff}/\varepsilon_0$)	$f = 0.896$ GHz at 25°C	0.036
	$f = 2.45$ GHz at 25°C	0.086
	$f = 10.6$ GHz at 25°C	0.452
	$f = 18.0$ GHz at 25°C	0.502
	Derivation: ref. [13]	

tively were used for the power dissipation. Without steel reinforcement, for microwave frequencies of 0.896 and 2.45 GHz, Type I mesh was used, while, for microwave frequencies of 10.6 and 18.0 GHz, Type II mesh was used. With the steel reinforcement, the Type II mesh was used for all calculations.

In the present analysis, three microwave applicator sizes, $D = 3.5$, 5.5 and 7.5 cm, with a 0.6 m thickness ($L = 0.6$ m) and a 2.0 m width ($2H = 2.0$ m) concrete block are considered. To ensure that the selection of H will not affect the temperature calculation, the ratio of the concrete width, H, to the microwave applicator size (D), H/D, remains larger than 25 ($H/D > 25$). It is confirmed from the result that the temperature variation in the direction of the concrete width is limited only in the range of $|y| < D$.

4. RESULTS AND DISCUSSION

The temperature distributions within a 0.6 m thick concrete slab with and without steel reinforcement, were analyzed. In the current analysis, a 25 cm by 25 cm mesh made by 2.5 cm diameter steel bars was considered. The corresponding value of the energy reflection (ρ_{sm}) from the steel reinforcement was then specified as 0.19. The location of the reinforcement (L_s) was also variable in the analysis, $L_s = 0.05$ and 0.1 m.

In the microwave industry, however, only some individual frequencies are available, for example, 0.896, 2.45, 10.6 and 18.0 GHz. These four commonly used microwave frequencies are utilized in the present discussion. The composition, and the dielectric and thermal properties of common concrete used in nuclear engineering are used and listed in Table 1.

According to the experiments reported in ref. [4], when the thermal stress and inner steam pressure exceeds the concrete tensile strength, the concrete near the front surface breaks into small debris in a depth of centimeters. The time of this spalling is about 60 s for $f = 2.45$ GHz with a microwave power intensity $Q_0 = 2.4 \times 10^6$ W m^{-2}, and the spalling time is about 15 s for $f = 10.6$ GHz with a $Q_0 = 8.0 \times 10^5$ W m^{-2}. Therefore, in the numerical calculation, the time limits for $f = 0.896$, 2.45, 10.6 and 18.0 GHz are set to 80, 60, 40 and 20 s, respectively.

4.1. *Microwave power dissipation*

The microwave power dissipation ($Q_{d,ave}$) is proportional to the effective dielectric loss (ε''_{eff}) and the square of the norm of the electric field potential (E_y). For different microwave frequencies (f), the microwave field pattern will be different even with the same geometry (L) and configuration (L_s, ρ_{sm}). In Fig. 3, the microwave power dissipations ($Q_{d,ave}L/Q_0$) for frequencies of 2.45 and 10.6 GHz within the concrete, with and without steel reinforcement, are presented. The power dissipation for $f = 0.896$ GHz is similar to that for 2.45 GHz, while the power dissipation for $f = 18.0$ GHz is similar to that for 10.6 GHz. Since the one-dimensional electromagnetic field model is used, the power dissipation within the dimensions of the microwave applicator ($|y| \leqslant D/2$) is assumed uniform.

4.2. *Temperature distributions*

As known, microwave power dissipation is the only source to cause the temperature to rises within the concrete. Consequently, the concrete temperature distributions and their variations depend on the geometry (concrete thickness, microwave applicator

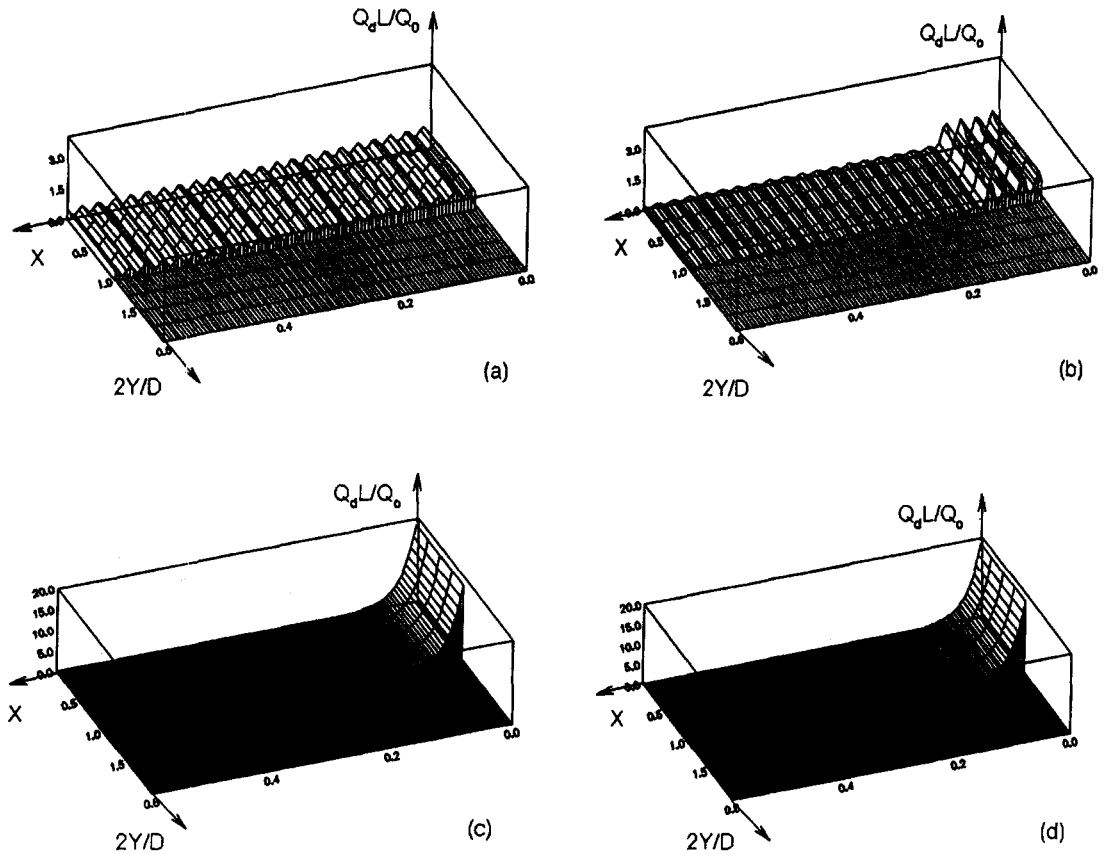

Fig. 3. Dimensionless microwave power dissipation ($Q_{d,ave}L/Q_0$) within a 0.6 m thick concrete slab with and without steel reinforcement located at $L_s = 0.1$ m: (a) $f = 2.45$ GHz without reinforcement; (b) $f = 2.45$ GHz with reinforcement; (c) $f = 10.6$ GHz without reinforcement and (d) $f = 10.6$ GHz with reinforcement.

size, etc.), behavior of the microwave power dissipation and the concrete thermal properties.

In the absence of reinforcement, the temperature distributions at a specified time for four microwave frequencies (0.896, 2.45, 10.6 and 18.0 GHz) are plotted in Fig. 4. It is shown in Fig. 4(a) that the shape of the temperature distribution for the frequency of 0.896 GHz is basically uniform in the y-direction. As frequency (f) increases, the shape of the temperature distribution is still similar to the power dissipation for $f = 2.45$ GHz, see Fig. 4(b). For a frequency lower than 2.45 GHz, the temperature distribution is wavy in the wave propagation direction. The peaks of the temperature distribution decay slowly along the propagation direction. Since the microwave at a low frequency has a large penetration distance within the material, the wave reflected from the concrete–air interface at the back surface has the same order as the propagating wave. The propagating and reflected waves compose a standing wave within the concrete slab. Therefore, the temperature distribution behaves wavy for low microwave frequencies ($f \leqslant 2.45$ GHz).

As frequency (f) further increases, $f \geqslant 10.6$ GHz, the shape of the temperature distribution changes. The wavy behavior of the temperature distribution disappears and is totally different from that for the $f \leqslant 2.45$ GHz. For the microwave at a higher frequency, for example $f = 10.6$ GHz, the penetration of the microwave drops dramatically. The wave amplitude diminishes after $x = 0.15$ m, which results in a very low power dissipation. Since the wave reflection from the back surface is almost negligible, no standing wave is formed within the concrete slab. Therefore, the power dissipation decreases sharply to zero along the x-direction. Similar to the power dissipation, the temperature distribution significantly varies from ambient temperature to the maximum temperature in a short distance and decays quickly. As seen in Fig. 4(c) and (d), only one peak appears on the temperature distribution for $f \geqslant 10.6$ GHz. The only temperature peak shifts more obviously toward the front surface. Therefore, the temperature near the front surface rises quicker than for the low frequencies, such as 0.896 and 2.45 GHz. Along the propagation direction, the temperature distribution drops dramatically, and, after $x > 0.1$ m, the temperature distribution is almost unchanged within $t = 20$ s.

Compared to the results for $f = 0.896$ GHz at $t = 60$ s, the maximum temperature $T_{max} = 37.6°C$. For $f = 2.45$ GHz with the same power intensity (Q_0) at

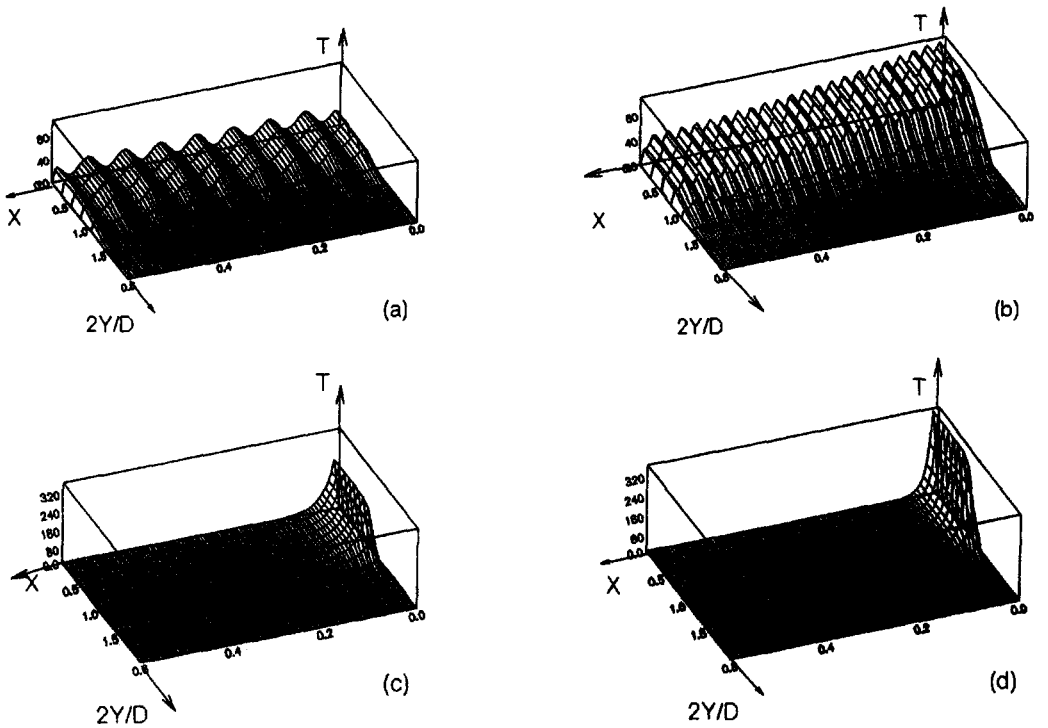

Fig. 4. Temperature distributions (T) within the concrete slab for $D = 5.5$ cm and for different microwave frequencies (f): (a) $f = 0.896$ GHz at $t = 60$ s; (b) $f = 2.45$ GHz at $t = 60$ s; (c) $f = 10.6$ GHz at $t = 15$ s and (d) $f = 18.0$ GHz at $t = 15$ s.

the same time (t) it is about 71.6°C, which is about 90% higher. For $f = 10.6$ GHz, it only needs 3.1 s to raise the maximum temperature (T_{max}) to the same value 71.6°C. For $f = 18.0$ GHz, the maximum temperature (T_{max}) shifts even closer to the concrete front surface than in the case for $f = 10.6$ GHz. The time needed to raise the same maximum temperature ($T_{max} = 71.6$°C) is only about 1.9 s.

In the concrete D&D process, it is very helpful to select the proper microwave frequency to control the position of the maximum temperature. Depending on the radioactive contamination history, precise control of the concrete spalling depth can keep the volume of the radioactively contaminated concrete to a minimum.

4.3. *Effect of microwave applicator size*, D

In addition to temperature variations in the wave propagation direction (x), the heat is also transferred in the direction of the microwave applicator width (or the y-direction). With different sizes of the applicator (D), the temperature pattern should be different. In Fig. 5(a) and (b), the temperature distributions for different values of D ($D = 3.5$ and 7.5 cm) with the same microwave power intensity ($Q_0 = 8.0 \times 10^5$ W m^{-2}) and frequency ($f = 2.45$ GHz) at the same time ($t = 60$ s), are plotted. The temperatures for $f = 10.6$ GHz, when $D = 3.5$ and 7.5 cm at $t = 15$ s, are presented in Fig. 5(c) and (d), respectively. Compared to Fig. 5(a) and (b), it is observed that, with the dimensionless y-axis ($2y/D$), the temperature patterns for two applicator sizes are almost identical except at the position close to the maximum temperature. The same behavior is also observed for $f = 10.6$ GHz and $t = 15$ s, see Fig. 5(c) and (d). Within the limit of the applicator size (or half size in the figures, $|y| \leqslant D/2$) in the y-direction, the temperature distribution is very flat, or nearly uniform.

It is well known that concrete is a very poor thermal conductor, and the thermal conductivity (k_{eff}) for most concrete is around 0.87 W m^{-2} K. During the concrete D&D process, the power intensity (Q_0) is kept to a very high level to minimize the concrete spalling time. Usually, Q_0 has a level of 8.0×10^5 W m^{-2} or higher. With such a high power intensity level, the temperature raises very quickly compared with the temperature diffusion in the y-direction. Therefore, with uniform heating in the y-direction, the heat transferred in that direction does not affect the temperature rise too much for this kind of high power intensity within such a short time ($t < 60$ s).

4.4. *Effect of the location of the steel reinforcement*

The steel reinforcement within the concrete structure might be located at different positions. For different locations of reinforcement (L_s), the temperature distributions will have different patterns. For a 0.6 m thick concrete slab with a reinforcement of 2.5 cm diameter bars on 25 cm center, vertically and horizontally ($\rho_{ms} = 0.19$ and $t_{ms} = 0.81$), located at

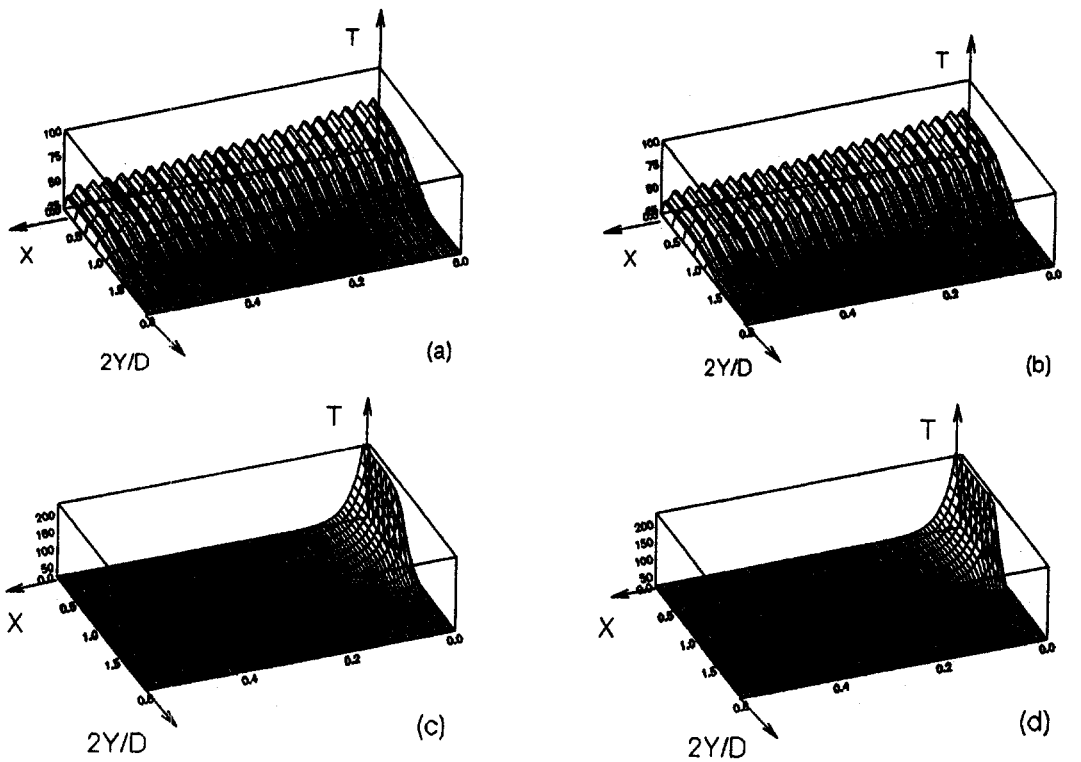

Fig. 5. Temperature distributions (T) within the concrete slab for $f = 2.45$ GHz and $f = 10.6$ GHz and for different microwave applicator sizes (D): (a) $f = 2.45$ GHz and $D = 3.5$ cm at $t = 60$ s; (b) $f = 2.45$ GHz and $D = 7.5$ cm at $t = 60$ s; (c) $f = 10.6$ GHz and $D = 3.5$ cm at $t = 15$ s and (d) $f = 10.6$ GHz and $D = 7.5$ cm at $t = 15$ s.

0.05 m and 0.1 m from the front surface, the temperature distributions for $f = 2.45$ GHz at $t = 60$ s and $f = 10.6$ GHz at $t = 15$ s are presented in Fig. 6(a)–(d), respectively.

For $f = 2.45$ GHz, the temperature distributions at $t = 60$ s with the steel reinforcement mesh located at $L_s = 0.1$ m and 0.05 m are plotted in Fig. 6(a) and (b). It is seen from the figures that the temperature drops dramatically after the reinforcement. With the presence of the reinforcement, an additional microwave is reflected when the wave interfaces with the steel mesh. This reflection with the propagating wave forms a stronger standing wave with a higher amplitude. After the reinforcement, since part of the energy is blocked by the steel mesh, the power dissipation is reduced. Therefore, the temperature is much lower than that without steel reinforcement and that between the front surface and the reinforcement. By comparing Fig. 6(a) with Fig. 5(b), it is found that the maximum temperature (T_{max}) of Fig. 6(a) is 86.2°C, while the maximum temperature (T_{max}) of Fig. 5(b), which has the same geometry but without reinforcement, is 71.6°C, approximately a 20% increase. As the reinforcement is located closer to the front surface, say $L_s = 0.05$ m, the maximum temperature (T_{max}) is almost the same as 86.2°C, see Fig. 6(b). This implies that with the presence of the steel reinforcement, a stronger standing wave with a larger amplitude will be formed between the reinforcement and the front surface of the concrete slab: thus, a higher maximum temperature (T_{max}) will be produced. When the reinforcement is located too close to the front surface, a large amount of reflected energy will be transferred through the layer between the reinforcement and the front surface, which is not totally dissipated within this layer.

The temperature distributions for $f = 10.6$ GHz at $t = 15$ s and $L_s = 0.1$ m and 0.05 m are presented in Fig. 6(c) and (d), respectively. It can be seen that the temperature distribution for $L_s = 0.1$ m is nearly the same as that without reinforcement. It is known from electromagnetic field analysis that the penetration of the microwave energy for $f = 10.6$ GHz is much less than that for $f = 2.45$ GHz, or the electric field (E_y) decays much faster as compared to that for $f = 2.45$ GHz. All microwave energy, except the reflection from the concrete front surface, is dissipated within a thickness of 0.15 m. Therefore, the presence of the steel reinforcement at $L_s = 0.1$ m slightly affects the temperature distributions, since the electric field (E_y) has already decayed to a very low level. For the case of $L_s = 0.05$ m, the temperature distribution is also similar to the case of $L_s = 0.1$ m. The only difference is that at $x = L_s$, the temperature has a sudden drop. The reason for this sudden drop is that part of the microwave energy is forced back between the front

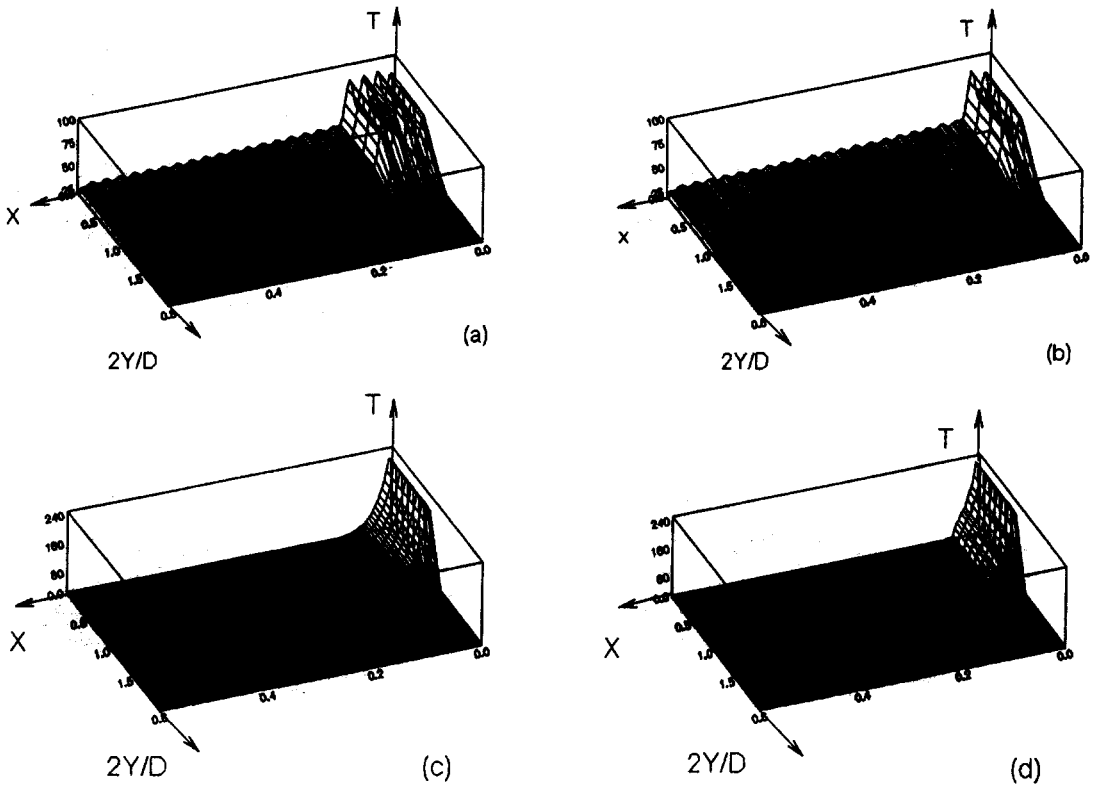

Fig. 6. Temperature distributions with the steel reinforcement ($\rho_{sm} = 0.19$) for $f = 10.6$ GHz: (a) $f = 2.45$ GHz, $\rho_{sm} = 0.19$ and $L_s = 0.1$ m at $t = 60$ s; (b) $f = 2.45$ GHz, $\rho_{sm} = 0.19$ and $L_s = 0.05$ m at $t = 60$ s; (c) $f = 10.6$ GHz, $\rho_{sm} = 0.19$ and $L_s = 0.1$ m at $t = 15$ s and (d) $f = 10.6$ GHz, $\rho_{sm} = 0.19$ and $L_s = 0.05$ m at $t = 15$ s.

surface and the steel reinforcement, which causes a sudden drop in the microwave power dissipation. Thus, there is not too much deviation between the maximum temperatures for $L_s = 0.1$ m and for $L_s = 0.05$ m, as presented in Fig. 6(c) and (d). It is concluded from Fig. 6 that the effect of the location of the steel reinforcement mesh on the temperature distributions for $f = 10.6$ GHz, or higher, will definitely be insignificant.

5. CONCLUDING REMARKS

Heat transfer and variation of the temperature distribution within a concrete slab exposed to a finite microwave heating source have been investigated. The effects of microwave frequency (f), the size of the microwave applicator (D) and the microwave reflection from the steel reinforcement (ρ_{sm}) located at $L_s = 0.05$ and 0.1 m have been discussed in the present paper. Based on the results and discussion, the following facts are concluded.

(1) Without any reinforcement, at a microwave frequency of $f \leqslant 2.45$ GHz, the temperature distribution displays a wavy behavior with an almost uniform amplitude. With the presence of the steel reinforcement, part of the microwave energy is reflected from the reinforcement, and more energy will be dissipated between the concrete front surface and the location of the reinforcement. The maximum temperature (T_{max}) increases dramatically.

(2) For a microwave frequency of 10.6 GHz, the temperature distributions are slightly affected by the presence of the steel reinforcement, since the penetration distance for this frequency is very small and most of the microwave energy is dissipated in a very short distance. The effect of the reinforcement for 10.6 GHz can be safely neglected.

(3) For a high power intensity, such as $Q_0 = 8.0 \times 10^5$ W m^{-2} or higher, the temperature variation within the dimensions of the microwave applicator is very small with uniform heating in that direction. The temperature rises very quickly compared with the temperature diffusion in that direction. Therefore, for different applicator sizes, the temperature patterns subject to uniform heating are almost identical.

Acknowledgement—The results presented in this paper were obtained in the course of research sponsored by the Department of Energy under Subcontract No. 19X-SM712V.

REFERENCES

1. A. Watson, *Microwave Power Engineering*, Vol. 2. Academic Press, New York (1968).
2. H. Yasunaka, M. Shibamoto and T. Sukagawa, Microwave decontaminator for concrete surface decontamination in JPDR, *Proceedings of the International Decommissioning Symposium*, pp. 109–115 (1987).
3. D. L. Hills, The removal of concrete layers from biological shields by microwave, EUR 12185, Nuclear Science and Technology, Commission of the European Communities (1989).
4. T. L. White, R. G. Grubb, L. P. Pugh, D. Foster, Jr. and W. D. Box, Removal of contaminated concrete surfaces by microwave heating—phase I results, presented at the 18th American Nuclear Society Symposium on Waste Management, Waste Management 92, Tucson, Arizona (1992).
5. W. Li, M. A. Ebadian, T. L. White, R. G. Grubb and D. Foster, Heat transfer within a radioactive contaminated concrete slab applying a microwave heating technique, *ASME Trans. J. Heat Transfer* **115,** 42–50 (1993).
6. W. Li, M. A. Ebadian, T. L. White, R. G. Grubb and D. Foster, Heat and mass transfer in a contaminated porous concrete slab subjected to microwave heating, *General Papers in Heat Transfer and Heat Transfer in Hazardous Waste Processing*, ASME HTD **212,** 143–153 (1992).
7. W. Li, M. A. Ebadian, T. L. White, R. G. Grubb and D. Foster, The effect of steel reinforcement on temperature and pressure within a porous concrete slab subjected to microwave heating, *Heat Transfer in Porous Media*, 1993 ASME HTD **240,** 1–10 (1993).
8. T. Z. Harmathy, Determining the temperature history of concrete constructions following fire exposure, *ACI Jl* **65,** 961–969 (1968).
9. G. A. Khoury, B. N. Grainger and P. J. E. Sullivan, Transient thermal strain of concrete: literature review, conditions within specimen and behavior of individual constituents, *Mag. Concr. Res.* **37,** 131–144 (1985).
10. J. R. Wait, *Electromagnetic Wave Theory*. Harper & Row, New York (1985).
11. A. N. Komarovski, *Shielding Material for Nuclear Reactors*. Pergamon Press, New York (1961).
12. I. Ursu, *Physics and Technology of Nuclear Reactors*. Pergamon Press, New York (1985).
13. M. A. Ebadian and W. Li, A theoretical/experimental investigation of the decontamination of a radioactively contaminated concrete surface using microwave technology, Final Report, DOE Project, DE-AC05-840R2140 (1992).